Robotica (2011) volume 29, pp. 787–796. © Cambridge University Press 2010
doi:10.1017/S0263574710000779

The elastic contact influences on passive walking gaits

Feng Qi†, Tianshu Wang†* and Junfeng Li‡

† *School of Aerospace, Tsinghua University, Beijing, 100084, P.R. China*
‡*Department of Engineering Mechanics, Tsinghua University, Beijing, 100084, P.R. China*

(Received in Final Form: November 5, 2010. First published online: December 2, 2010)

SUMMARY
This paper presents a new planar passive dynamic model with contact between the feet and the ground. The Hertz contact law and the approximate Coulomb friction law were introduced into this human-like model. In contrast to McGeer's passive dynamic models, contact stiffness, contact damping, and coefficients of friction were added to characterize the walking model. Through numerical simulation, stable period-one gait and period-two gait cycles were found, and the contact forces were derived from the results. After investigating the effects of the contact parameters on walking gaits, we found that changes in contact stiffness led to changes in the global characteristics of the walking gait, but not in contact damping. The coefficients of friction related to whether the model could walk or not. For the simulation of the routes to chaos, we found that a small contact stiffness value will lead to a delayed point of bifurcation, meaning that a less rigid surface is easier for a passive model to walk on. The effects of contact damping and friction coefficients on routes to chaos were quite small.

KEYWORDS: Passive dynamic; Hertz contact law; Approximate Coulomb friction law; Chaos; Gait.

1. Introduction

Fallis[1] was the first to build a passive dynamic walking model. McGeer[2,3] first introduced the concept of planar passive dynamic walking models and built a class of prototypes. Later, Garcia[4] and Goswami[5] studied simple compass-like planar passive walking locomotion, and their research confirmed that a steep ramp slope leads to bifurcation of the walking gait. These results were supported by Kurz *et al.*[6] using the largest Lyapunov exponent and surrogate analysis methods. Until now, the types of passive dynamic models varied from 2D to 3D, from simple to complex, and the research varied from simulations to experiments. An uncontrolled 3D passive walking model was first made by Coleman *et al.*[7] Kuo's work[8] on extending the planar passive walking model to allow for the roll motion confirmed that this motion is unstable. A model using a pelvic body as the passive dynamic compensator was designed by Wisse *et al.*[9] to stabilize the yawing and rolling motions. Collins *et al.*[10] successfully built the first 3D two-legged passive-dynamic machine with knees. Narukama *et al.*[11] later replaced the arc-shaped feet with flat feet in their simple 3D model. Compared to other 3D models, a complex planar model is easier to study. Wisse[12] established the simplest model with an upper body. His research showed that the presence of the upper body results in better energy efficiency and robustness. Safa *et al.*[13] replaced the ramp slope with stairs using Garcia's model, and found that the ramps have more ability for generating stable walking. Ning[14] conducted a systematic study of the gait of a straight leg model through simulations and experiments. All of these passive-biped models mentioned above can walk with less dissipation of energy than traditional robots, such as the Honda Asimo[15] because of their human-like walking gaits.

Improving a human-like walking model requires paying special attention to the upper body, the hip, the leg formation, the control laws, and the feet. The shape of the feet and the collision of the feet are important in passive walking. To our knowledge, an elastic contact model has never been used to analyze passive walking. The collisions in most of the models simulated above are rigid plastic collisions (no-slip and no-bounce). We estimate that elastic contact will significantly affect passive walking gaits.

The main aim of our research is to incorporate a more detailed contact into passive walking to work out the contact influence on walking gaits. The elastic contact between the ramp and the feet was examined using the Hertz contact law and the approximate Coulomb friction law.

2. Model with Non-Plastic Contact

The model we considered was based on the planar model with straight legs and round feet. The contact laws acted on the round feet and the ground. The normal contact force (the Hertz contact model) and tangential contact force (the approximate Coulomb friction model) acted on the point when contact occurred.

2.1. Hertz contact law

In a rigid multi-body Newtonian system, the impulse of the contact force is used to define the recovery coefficient. The contact duration is set to be zero, so the impaction takes place and finishes instantly. It is not difficult to calculate the kinematic parameters, but the contact force cannot be derived from the process.

An elastic model is needed to calculate the contact force. In 1882, Hertz worked on the contact between two elastic semi-infinite solids. His work is summarized by Johnson.[16] The Hertz contact model showed that the elastic contact force is proportional to the three-halves power of the imbedded depth

* Corresponding author. E-mail: tswang@tsinghua.edu.cn

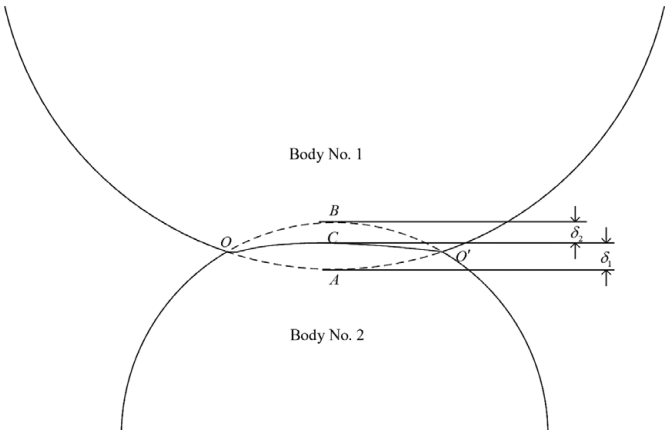

Fig. 1. As shown above, OAO' is the outline of Body No.1 with no deformation, and OBO'. is the outline of Body No. 2 with no deformation. OCO' is the contact line when the two bodies contact and paste with each other.

of the elastic body. We introduced this Hertz elastic contact force and a damping contact force into the passive dynamic walking model to simulate the inelastic collision with energy cost. Suppose $\delta = \delta_1 + \delta_2$ is the imbedded depth of the two contact bodies, as shown in Fig. 1.

The expression of the normal contact force can be written as follows:

$$\begin{cases} N = 0 & \text{if} \quad \delta \le 0 \\ N = k\delta^{3/2} - c\delta^{3/2}\dot{\delta} & \text{if} \quad \delta > 0 \end{cases}.$$

Usually we let $k = 10^6 \text{kgm}^{-1/2}\text{s}^{-2}$ and $c = 10^7 \text{kgm}^{-3/2}\text{s}^{-1}$, and the collision occurs as the perfect inelastic collision. If we let $c = 0$, the collision becomes the perfect elastic collision. Therefore, parameter c is the elasticity of the foot and the ground and parameter k is the rigidity of the foot and the ground.

2.2. *Friction law*

The Coulomb friction force is proportional to the normal pressure: $f = \mu N$. The friction coefficient μ is a non-smooth function of tangential relative velocity (Fig. 2). When relative velocity is not zero, the coefficient of friction and the relative velocity have opposite signs, and the kinetic friction coefficient is $\pm\mu_s$; when the relative velocity is zero, the friction is static and the coefficient is a multivalued function, which varies from $-\mu_d$ to $+\mu_d$. Usually, such a non-smooth multi-body system is difficult to integrate numerically, so we replaced the non-smooth part of the Coulomb friction curve with several cubic functions (Fig. 2) from MSC-ADAMS (a multi-body system simulation software).[17] In our simulation below, these two relative velocities of friction coefficients are chosen as $v_s = 10^{-4}$, $v_d = 10^{-3}$, and these are small enough for our approximation to the Coulomb friction law.

When the tangential relative velocity of the contact point is v_t, the expressions of friction force are as follows:

$$\begin{cases} f = \mu_d N & \text{if} \quad v_t \le -v_d, \\ f = \left[\mu_d + (\mu_s - \mu_d)\left(\frac{v_t+v_d}{v_d-v_s}\right)^2\left(3 - \frac{2(v_t+v_d)}{v_d-v_s}\right)\right] N & \text{if} \quad -v_d \le v_t \le -v_s, \\ f = \left[\mu_s - 2\mu_s\left(\frac{v_t+v_s}{2v_s}\right)^2\left(3 - \frac{v_t+v_s}{v_s}\right)\right] N & \text{if} \quad -v_s \le v_t \le v_s, \\ f = \left[-\mu_s + (\mu_s - \mu_d)\left(\frac{v_t-v_s}{v_d-v_s}\right)^2\left(3 - \frac{2(v_t+v_s)}{v_d-v_s}\right)\right] N & \text{if} \quad v_s \le v_t \le v_d, \\ f = -\mu_d N & \text{if} \quad v_t \ge v_d. \end{cases}$$

2.3. *Equation of motion*

The model we analyzed is a planar passive dynamic walking model with round feet and straight legs. The general view of the model is shown in Fig. 3. O' is the position of hip; C_1 and C_2 are the positions of two legs' center of mass; D_1 and D_2 are the lowest points of both feet, referred to as the potential impact points. The parameters of the model are listed as follows: l_1 and l_2 are the length of two legs; m_1 and m_2 are the mass of two legs; J_1 and J_2 are the moments of inertia to the mass center of two legs; r_1 and r_2 are the radii of two round feet; c_1 and c_2 are the distance between hip and the mass center of two legs; γ is the ramp slope; and g is the acceleration of gravity.

During the walking process, the two feet are imbedded in the ground, so the model has four degrees of freedom. We set the OXY axis fixed on the ramp; the X direction moves horizontally along the ramp and the Y direction moves away vertically from the ramp. The four generalized coordinates can be chosen as x_0, y_0, θ_1, θ_2. The equations of motion are

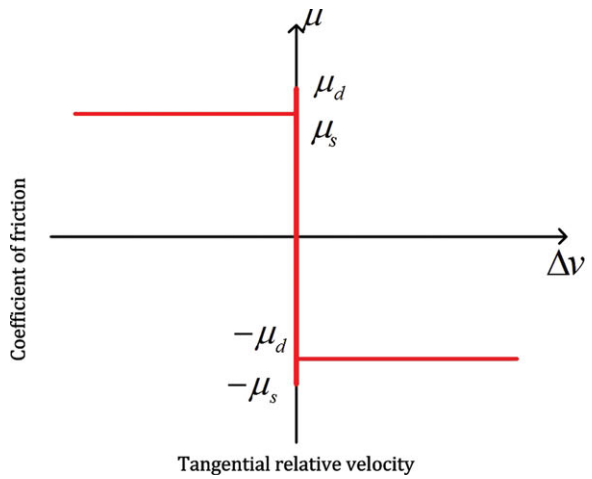

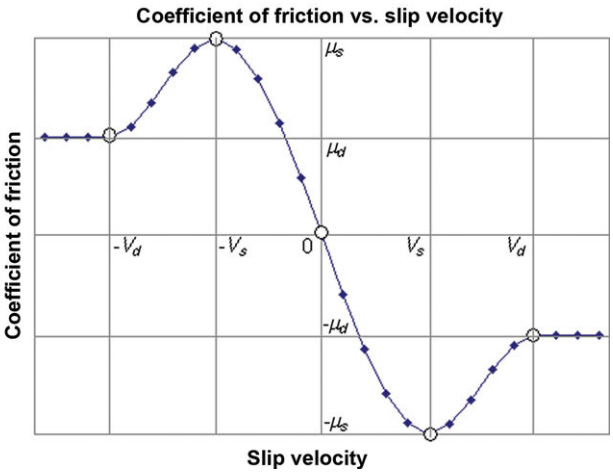

Fig. 2. Coefficient of friction in Coulomb model and approximate Coulomb model.

https://doi.org/10.1017/S0263574710000779 Published online by Cambridge University Press

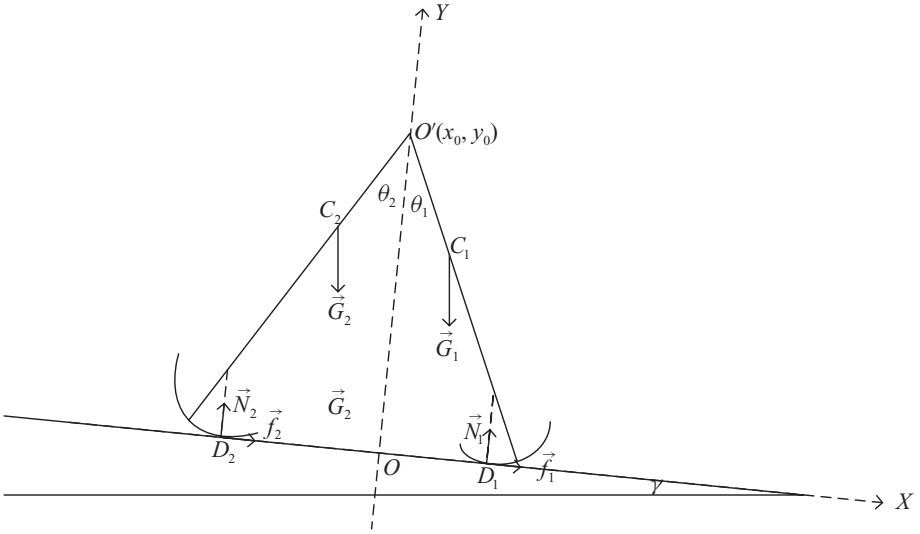

Fig. 3. Passive dynamic walking model with contact.

derived using Lagrange formulation

$$\begin{cases} (m_1+m_2)\ddot{x}_0 + m_1c_1\ddot{\theta}_1\cos\theta_1 + m_2c_2\ddot{\theta}_2\cos\theta_2 \\ \quad -m_1c_1\dot{\theta}_1^2\sin\theta_1 - m_2c_2\dot{\theta}_2^2\sin\theta_2 = (m_1+m_2)g\sin\gamma \\ \quad +f_1+f_2 \\ (m_1+m_2)\ddot{y}_0 + m_1c_1\ddot{\theta}_1\sin\theta_1 + m_2c_2\ddot{\theta}_2\sin\theta_2 \\ \quad +m_1c_1\dot{\theta}_1^2\cos\theta_1 + m_2c_2\dot{\theta}_2^2\cos\theta_2 = -(m_1+m_2)g\cos\gamma \\ \quad +N_1+N_2 \\ m_1c_1^2\ddot{\theta}_1 + m_1c_1\ddot{x}_0\cos\theta_1 + m_1c_1\ddot{y}_0\sin\theta_1 + J_1\ddot{\theta}_1 \\ \quad = -m_1gc_1\sin(\theta_1-\gamma) + N_1(l_1-r_1)\sin\theta_1 \\ \quad\quad +f_1[(l_1-r_1)\cos\theta_1 + r_1] \\ m_2c_2^2\ddot{\theta}_2 + m_2c_2\ddot{x}_0\cos\theta_2 + m_2c_2\ddot{y}_0\sin\theta_2 + J_2\ddot{\theta}_2 \\ \quad = -m_2gc_2\sin(\theta_2-\gamma) + N_2(l_2-r_2)\sin\theta_2 \\ \quad\quad +f_2[(l_2-r_2)\cos\theta_2 + r_2] \end{cases}.$$

N_i and f_i are the contact forces of both feet; these forces apply on the lowest point of the feet, which are D_1 and D_2 in our model. As the lowest points on the feet change, the points of application of the contact forces also change. The expressions for imbedded depth δ and contact point tangential relative velocity v_t are written as follows:

$$\begin{cases} \delta_i = -y_{Di} = -y_0 + (l_i - r_i)\cos\theta_i + r_i \\ v_{ti} = \dot{x}_{Di} + r_i\dot{\theta}_i = \dot{x}_0 + (l_i - r_i)\dot{\theta}_i\cos\theta_i + r_i\dot{\theta}_i \end{cases} \quad i = 1, 2.$$

The contact forces can be derived from the equations given in Sections 2.1 and 2.2 by using δ and v_t. The equations of motion contain the normal contact and friction forces, so these are not easy to write in dimensionless form. In all forthcoming sections, we will describe equations and parameters using the SI units.

2.4. The walking procedure in programming

The form of the motion equations listed above remains the same when the model is walking. The transition rules when the swing foot hits the ground are no longer needed in this model. N_i and f_i need to be changed during the integration progress. We mark each leg as a swing leg or a stance leg in a walking cycle. The contact forces can only be applied to a stance leg. A swing leg swings forward with no contact forces, so foot scuffing is neglected. In our model $\delta_i = -y_{Di} = -y_0 + (l_i - r_i)\cos\theta_i + r_i$, which defines the distance between the lowest point of the feet and the ground. We use this distance to change the legs' roll in the program,

$$\begin{cases} \textit{stance leg} \rightarrow \textit{swing leg when } \delta > 0 \;\&\; \dot{\delta} > 0 \\ \textit{swing leg} \rightarrow \textit{stance leg when } \delta < 0 \;\&\; \dot{\delta} < 0 \end{cases}.$$

In the program for simulating the passive dynamic walking model, a subfunction is used to estimate which legs are stance legs.

3. Simulation and Discussion

3.1. Finding stable period-one gait cycles

The stable period-one gait cycles exist under different model parameters, if the right initial condition is given. The parameters of a period-one walking cycle are listed in Table I. The units used are international units. Gravity acceleration g is 9.8 ms^{-2}. Initial condition q_0 contains eight parameters listed in the last line of the table. The first four parameters of initial condition q_0 represent No. 1 leg's initial angle, No. 2 leg's initial angle, and the initial coordinates of the hip (x_0, y_0). The next four parameters of q_0 represent the derivatives of the first four parameters.

The stable period-one gait cycles can be found under the above conditions. The initial condition is guess based on Liu's results.[14] The plots of leg angles over two cycles are shown in Fig. 5. Both legs' angles versus time are periodic. The motion of both legs is same because the model is symmetric, and the second leg's angle is a half-cycle delayed from the first leg's angle.

Figure 6 shows the contact forces over time in one cycle. The left figure shows the normal contact force and the right figure shows the tangential contact force. For one cycle in the left figure, the force magnitude becomes comparatively large in the beginning of the contact. The force peaks only for an instant, and remains at the value of gravity during

https://doi.org/10.1017/S0263574710000779 Published online by Cambridge University Press

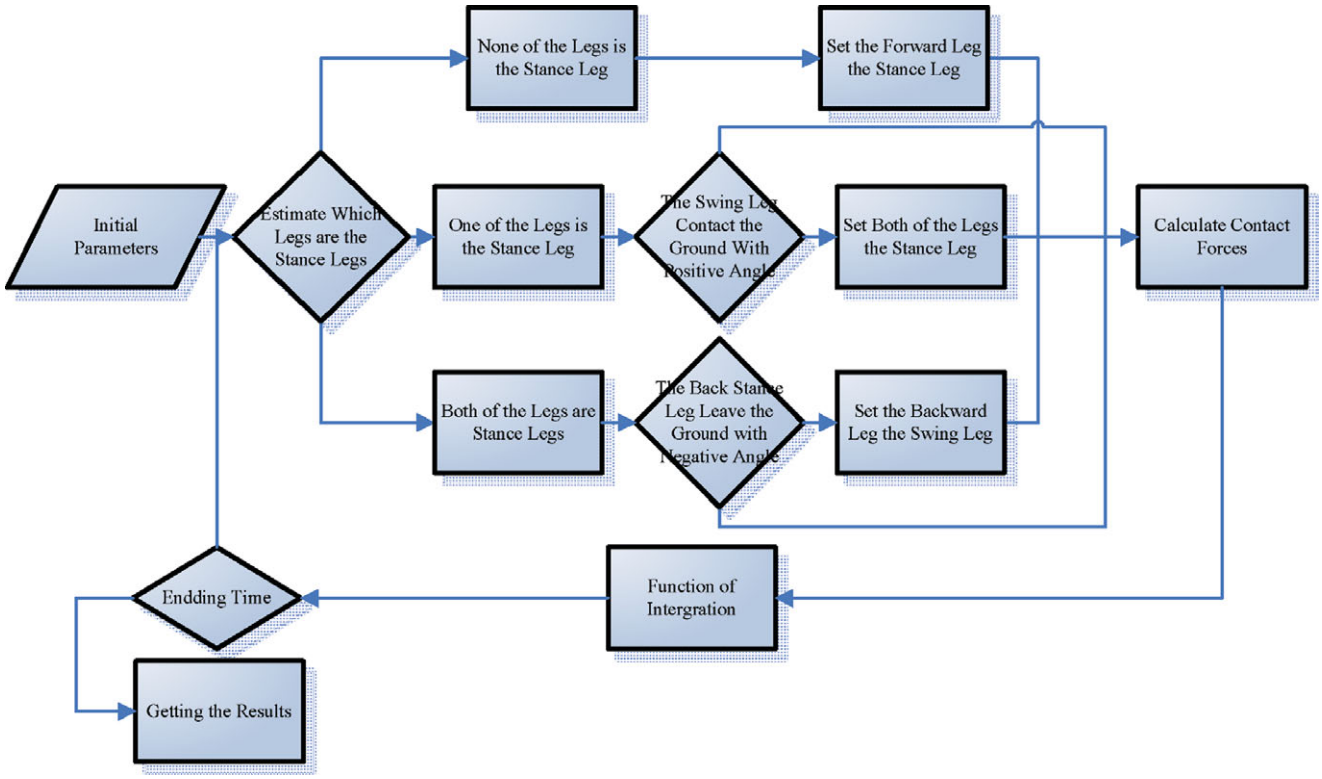

Fig. 4. Outline of the program. When the model is walking, at least one leg is a stance leg. The function is stiff, so ode23s in MATLAB® is used to integrate these equations.

most of the remainder of the contact period. The wave in the beginning of the contact is the force in an impact period; the smooth force represents the rotating period of the stance leg. For one cycle in the right figure, the magnitude of the force becomes comparatively negative at the beginning and end of the contact. In the rotating period, the friction changes from negative to positive as the foot moves forward to backward. Here the friction is the same as it is in human walking.

When the initial condition q_0 is set to $q_0 + \delta q_0$, the walking gait will converge to the same cycle if δq_0 is adequately small. The period-one gait cycle is stable in this example.

3.2. *Period doubling and passive dynamic staggering*

Period doubling occurs in Garcia's[4] model when the ramp slope is sufficiently steep. This is also true for our complex model. The parameters of the period-two gait cycle are listed in Table II.

The angles of both legs versus time and phase diagram are shown on the left side in Fig. 7. The normal contact force over time is shown on the right side in Fig. 7. The left figure indicates that both legs' angles versus time are periodic, but

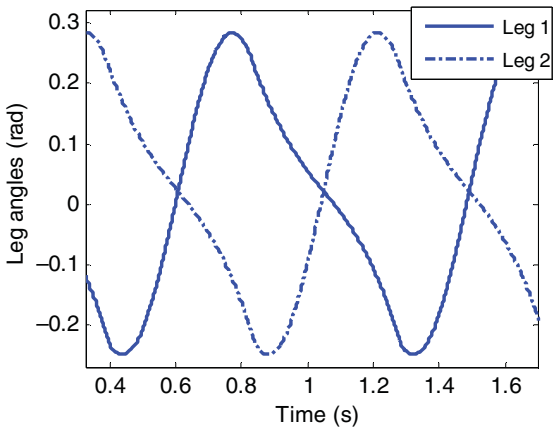

Fig. 5. Leg angles and leg phase diagram over several steps.

their gaits are different. Under these parameters the model is symmetric, but the gait is not. This result is the same as that from Garcia's passive dynamic staggering.[4] The right figure shows the normal contact forces of the two feet versus time. In the passive dynamic staggering, the peak values of both

Table I. The parameters and initial conditions of a stable period-one gait cycle.

Model parameters	m_i	l_i	c_i	r_i	J_i	γ		
	1	0.4	0.1	0.08	0.0096	0.02		
Contact parameters	k	c	v_s	v_d	μ_s	μ_d		
	10^6	10^7	10^{-4}	10^{-3}	0.5	0.4		
Initial conditions	θ_1	θ_2	x_0	y_0	ω_1	ω_2	v_{x0}	v_{y0}
	0.1655	−0.2479	0	0.3950	−1.2565	0.0052	0.4971	0.0486

https://doi.org/10.1017/S0263574710000779 Published online by Cambridge University Press

Table II. The parameters of period-two gait cycles with higher γ to 0.11 radians.

Model parameters	m_i	l_i	c_i	r_i	J_i	γ		
	1	0.4	0.1	0.08	0.0096	**0.11**		
Contact parameters	K	c	v_s	v_d	μ_s	μ_d		
	10^6	10^7	10^{-4}	10^{-3}	0.5	0.4		
Initial conditions	θ_1	θ_2	x_0	y_0	ω_1	ω_2	v_{x0}	v_{y0}
	0.3893	−0.4109	0	0.3737	−2.1141	0.6477	0.7951	0.3162

feet's normal force are not the same. The peak force of the leg with a larger swing angle is smaller.

3.3. Influence of contact parameters on walking gaits

In our model, the relationship between model parameters and walking gait (Table III) is the same as in Ning's[14] results. However, the results of the influence of contact parameters on walking gaits have not been demonstrated in any previous research.

3.3.1. Hertz contact stiffness. The Hertz contact stiffness represents the rigidity of the ground and the feet. With a higher value of contact stiffness, the deformation of the impact on the ground decreases (the rigidity of iron is much higher than wood). Humans walk differently on different surfaces, and so will the passive dynamic model. The effects

Table III. The model parameters' effects on walking speed.

	Step length	Period	Speed
$c\uparrow$	↓	↓	↓
$J\uparrow$	↑	↑	↓
$r\uparrow$	↑	↑	↑

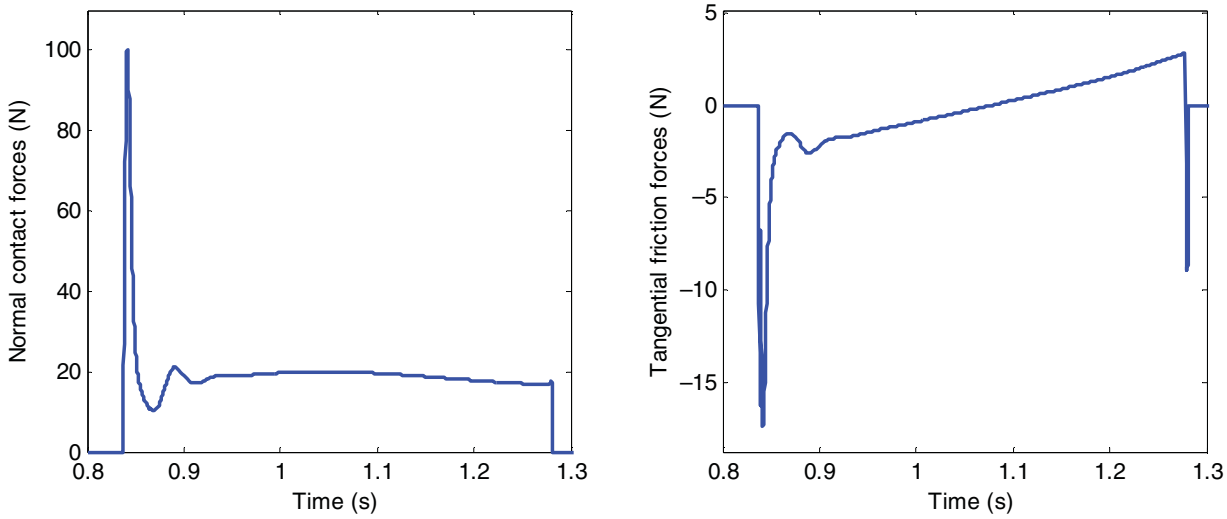

Fig. 6. Contact force on foot 1 over one gait.

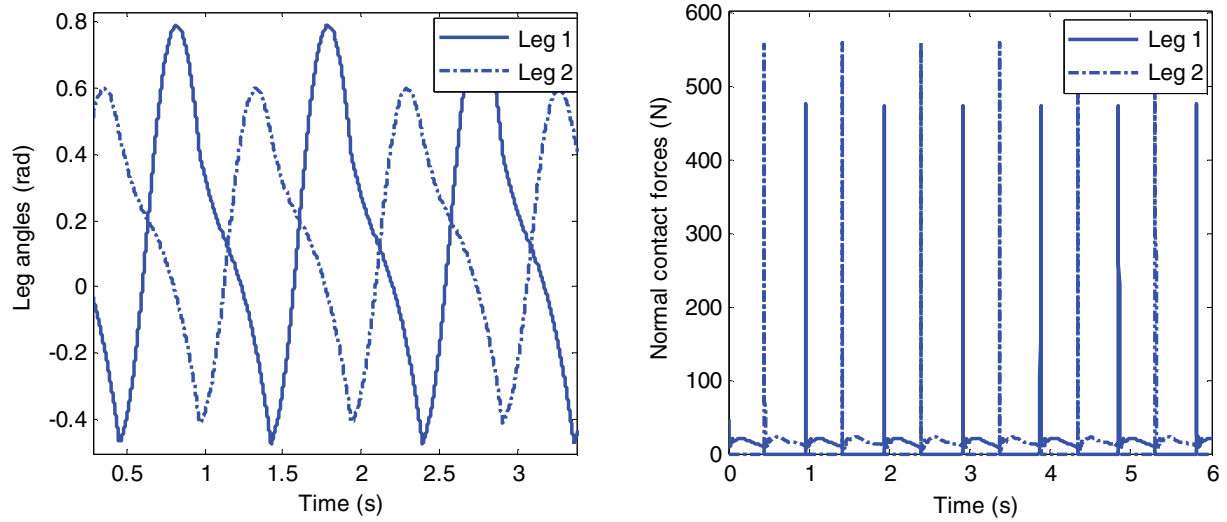

Fig. 7. Period doubling on a steeper ramp slope.

https://doi.org/10.1017/S0263574710000779 Published online by Cambridge University Press

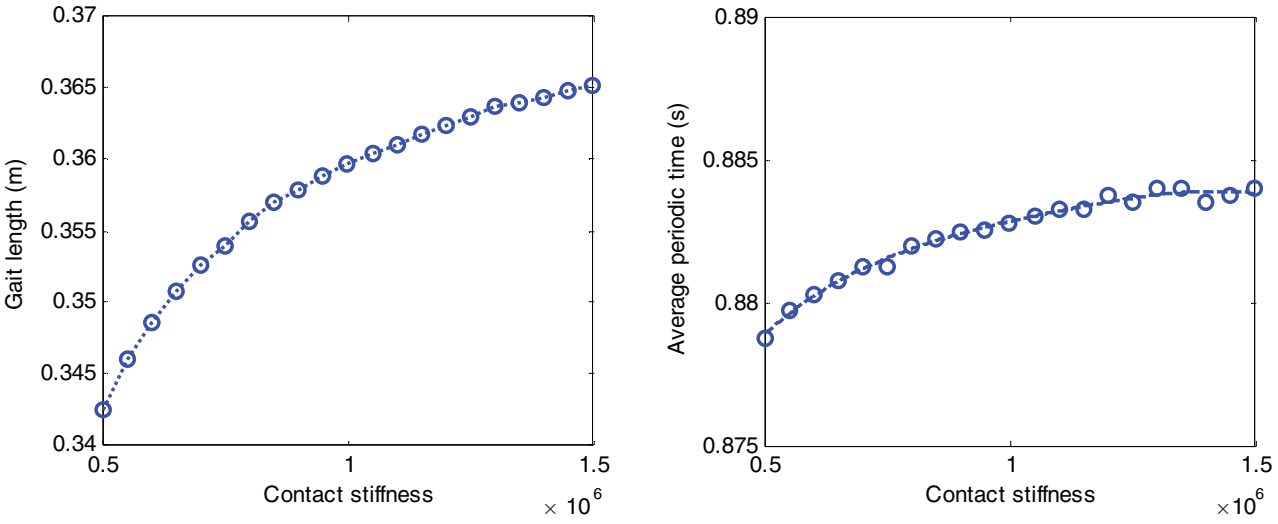

Fig. 8. The gait length and average period increase as the contact stiffness increases. The increase of the period is much smaller than that of the gait length, so the changes in periodic time can be ignored here.

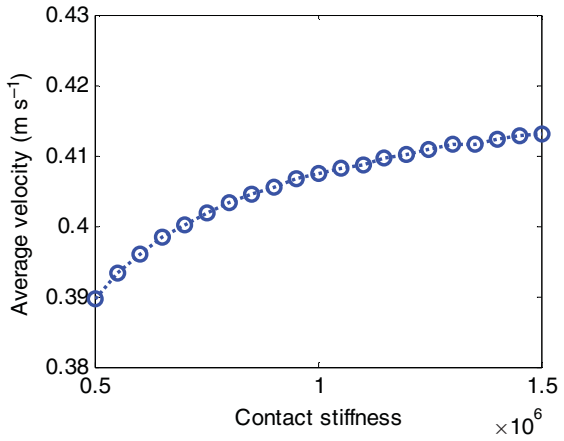

Fig. 9. The effects of contact stiffness on average velocity.

of contact stiffness on the walking gait length, period, and average speed of hip are listed below. The average speed is the average speed of hip in X direction in several stable period-one walking trials.

The contact stiffness changes from 0.5×10^6 to 1.5×10^6. The contact damping and coefficients of friction are the same as those in the period-one example in Section 3.1. From the simulations, the effect of contact stiffness on walking gaits is obvious. The length of walking gaits (Fig. 8) and average velocity (Fig. 9) rises with increasing stiffness. The changes of contact stiffness from 0.5×10^6 to 1.5×10^6 can increase the average velocity and the length of walking gaits by about 5%. A passive biped walking model slows down on a soft ground just like humans. The global characteristics of walking change with different values of contact stiffness, including the area of the phase diagram, the period of the gait, and the peak of the normal contact force.

3.3.2. Contact damping. The Hertz contact damping represents the elasticity of the ground and the feet. With a value of the contact damping large enough, the feet have no-bounce collisions with the slope surface. If the contact damping decreases to a sufficiently low value, the collision of the feet and the ground will lead to a large vertical vibration, and the model will fall down.

In this example, the effects of contact damping on walking gaits are simulated. The contact damping varies from 1.6×10^6 to 2.6×10^6. The contact stiffness and coefficients of friction are the same as in the period-one example from Section 3.1. It is clear from the simulation that the effects of contact damping on walking gaits are insignificant. A model's walking gaits do not change after the contact damping increases to a large value, whereas with a very small value the model will not be able to walk. The average velocity decreases as the contact stiffness increases (Fig. 11). The changes of contact damping from 1.6×10^6 to 2.6×10^6 can increase the average velocity and the length of walking gaits (Fig. 10) by about 2.5%. Less contact damping leads to contact with more bounces, and the forward inertia makes the model walk fast. The global characteristics of walking do not change with different contact stiffness values.

3.3.3. Friction parameters. The following two coefficients of friction are used in the approximate Coulomb friction law: the kinetic friction coefficient and the max static friction coefficient. Usually, the max static friction coefficient is larger than the kinetic friction coefficient. In simulations, we consistently altered the two coefficients. As in the period-one example given in Section 3.1, the walking gait changes can be neglected when there is an increase in friction coefficients. On the other hand, the fall in friction coefficients decreases the model's stability. When we decrease μ_s to 0.3 and μ_d to 0.2, the swing leg slips on the slope and collision occurs (Fig. 12). When $\mu_s = 0.2$ and $\mu_d = 0.1$, the ground is too smooth for the model to walk.

3.4. Period doubling and routes to chaos

Both Garcia[4] and Goswami[5] observed period doubling in stable walking motions when the slope angle is increased. Ning's[14] model with round feet also experienced period

https://doi.org/10.1017/S0263574710000779 Published online by Cambridge University Press

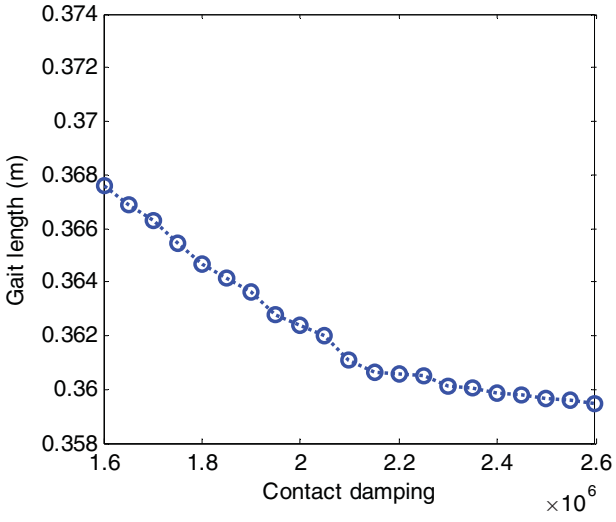

Fig. 10. The gait length decreases as the contact damping increases. When the contact damping is large enough for no-bounce contact, the gait length will not change. The contact damping has almost no effect on the period.

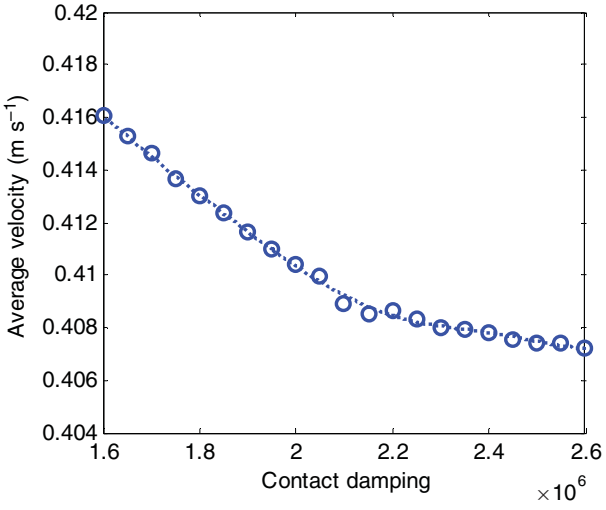

Fig. 11. The effects of contact damping on average velocity.

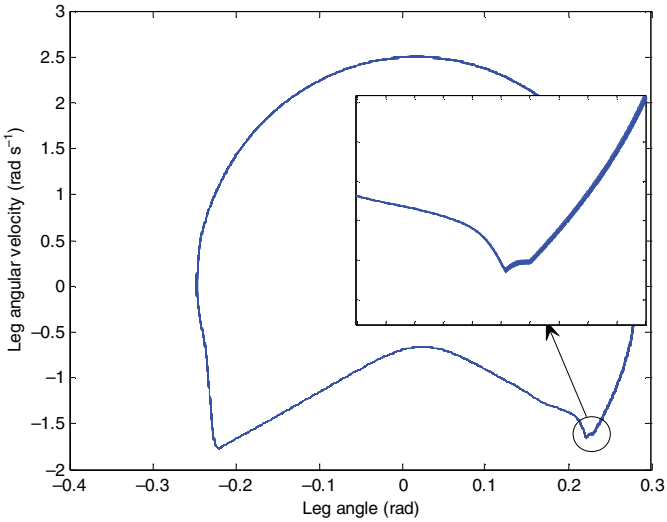

Fig. 12. The stable walking gait with slipping. The inset shows the enlarged view of the contact procedure. When the coefficients of friction decrease to certain values, the foot slips on the ground as the collision of the swing leg and the ground occurs. When the friction coefficients are large enough for the model to walk, the global characteristics of walking do not change with different coefficients.

doubling as this model's parameters are changed. Similarly, our complex model also experiences the same phenomenon as the slope angle increases. The graph of period doubling is shown in Fig. 13. Some new results are derived here by changing the contact parameters.

3.4.1. Contact stiffness and routes to chaos. With constant contact damping, friction coefficients, and model parameters, the period doubling (Fig. 13) changes in a regular pattern according to different values of contact stiffness. In Garcia's simplest walking model, bifurcation happens when γ is more than 0.015 radians,[4] which is quite less than the value of γ in our model. In contrast, for different values of contact stiffness, we found that bifurcation starts at a smaller ramp slope as contact stiffness increases. The contact stiffness in the plastic collision seems infinitely large, so the bifurcation happens with a much smaller γ.

In Garcia's results, no persistent gait was found on slopes much steeper than 0.019 radians. But in our model, the gait is stable at a much steeper slope because the values of the contact stiffness are much smaller.

3.4.2. Contact damping and routes to chaos. In the same way, period doubling for different values of contact damping is shown in Fig. 14, with contact stiffness and friction coefficients being constant. We found that the contact damping has little to do with bifurcation points, but the collision liberation cannot be neglected with a small contact damping value. A small contact damping value implies the presence of legs with nonlinear spring, and the stance leg

https://doi.org/10.1017/S0263574710000779 Published online by Cambridge University Press

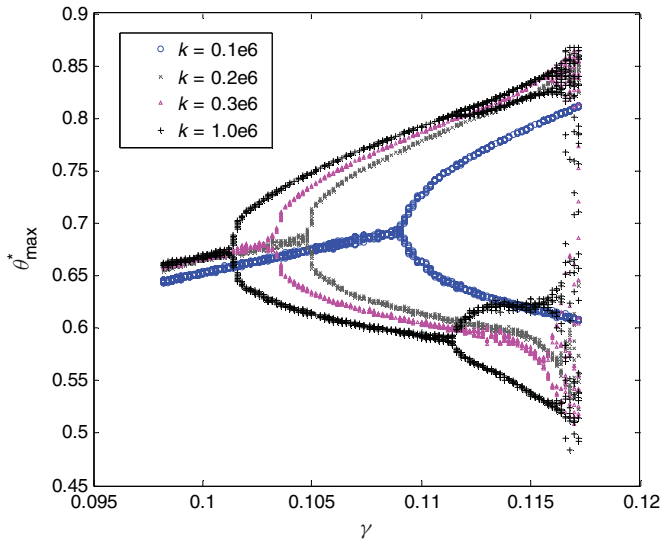

Fig. 13. Four models with different values of contact stiffness were computed numerically, and the results for different contact stiffness show that the period doubling point occurs much later. Lower contact stiffness implies a softer surface or feet, so a softer contact with the ground will delay period doubling.

will bounce like the flight and passive running in McGeer's model.[18]

3.4.3. Friction coefficients and routes to chaos. In the approximate friction law, the kinetic friction coefficient is smaller than the max static friction coefficient, so the two friction coefficients must be changed together. The period doubling for different values of friction coefficients is shown in Fig. 15.

In Wu's experimental study,[19] the 3D walking device could walk with a smaller minimum ramp angle and a smaller friction coefficient. Similarly, in this model, the walker can walk with a larger ramp angle and larger friction coefficients. As for the walking speed and energy dissipation are concerned, the contact parameters are related to natural materials, so it is difficult to calculate the relationship between energy dissipation and friction coefficients.

4. Conclusions

This paper presented a complex passive walking model with straight legs and round feet. The Hertz contact law and the approximate Coulomb friction law were considered in this model. Examples with period-one and period-two gait cycles were derived from this walking model. The contact forces could also be calculated from the numerical simulation.

The effects of changing contact parameters on walking gaits are summarized in Table IV. The results of variation of model parameters on walking gaits are the same as in Ning's results.[14]

From the above discussion we conclude the following:

(a) A lower contact stiffness corresponds to soft feet or a soft surface. The walker walks more slowly and more steadily on a softer ramp.
(b) Lower contact damping corresponds to elasticity. This parameter has little connection with the route to chaos. It represents the vibration of collision. For a small contact damping value, the movement looks like jumping.
(c) The friction coefficients' influence is limited to the slipping of the feet. If the friction is too small, the feet slip on the ground. It is not connected with the route to chaos, but shows when bifurcation stops in the diagram.
(d) The effects of contact parameters changes on walking gait are related to the energy dissipation. For the higher energy

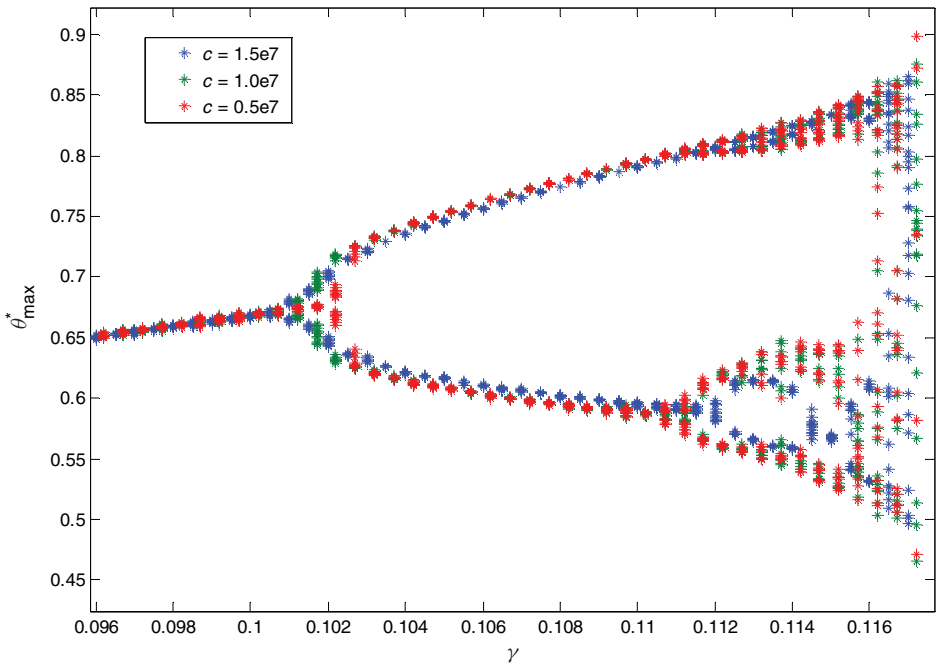

Fig. 14. The influence of contact damping on the routes to chaos. Comparing the period doubling route to chaos under the three contact damping parameters, we conclude that contact damping has little effect on the route to chaos and the stability of walking. However, the contact damping will certainly affect walking characteristics like the initial condition or vibration during walking cycles.

https://doi.org/10.1017/S0263574710000779 Published online by Cambridge University Press

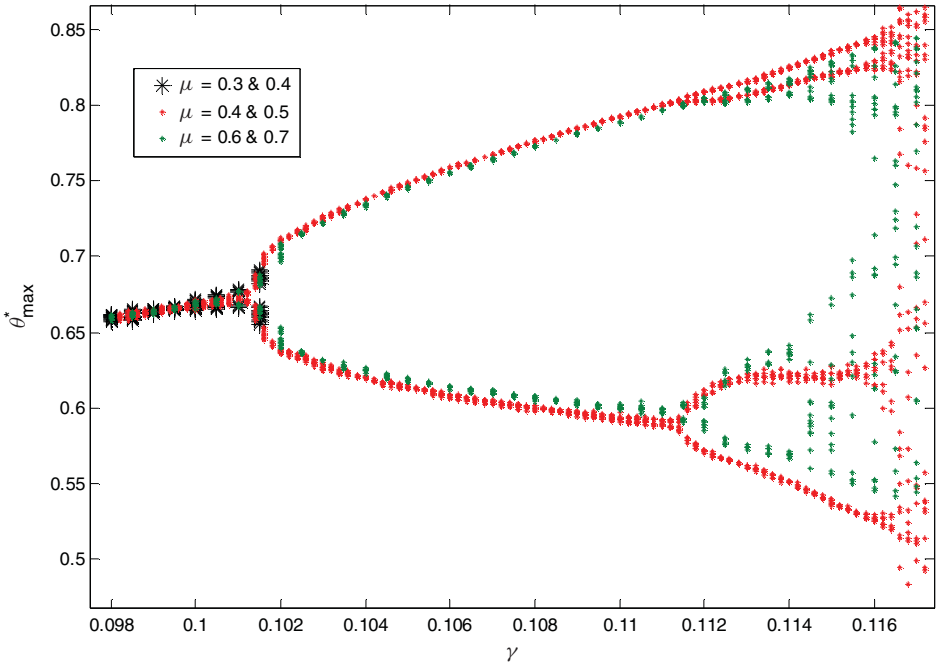

Fig. 15. Models with three pairs of friction coefficients are simulated here. The model cannot walk when the ramp is steeper than 0.102 radians because the friction coefficient is too small for the walker to stick to the surface. For the models with friction coefficients large enough to be able to walk, friction has no effect on period doubling.

Table IV. Effects of contact parameters on gait. ↑ represents increasing, ↓ represents decreasing, – represents an invisible change. Note the last row. with friction coefficients below certain level, the feet will slip on the ramp and the model will not be able to walk.

	Step length	Period	Speed	Bifurcation point
When k ↑	↑	↑	↓	Advanced
When c ↑	↓	–	↓	–
When μ ↑	–	–	–	–

cost, the walking length is larger. This means the contact stiffness changes the energy cost in the walking period, while the contact damping and the friction coefficients have no effect.

(e) The bifurcation of walking gait has some connection with the walking speed. Bifurcation occurs when the speed is sufficiently high. This is similar when an adult is leading a child to walk: the child's walking becomes chaotic and it is easy for the child to fall down if the leading speed is fast.

In the future studies, the contact laws can be extended to 3D models, as the friction and collision in these models are very important. We expect to conduct such experiments in the upcoming phases of our research. The contact forces can then be compared with the experimental results.

Acknowledgments

This research is funded by the National Natural Science Foundation of China (10872102).

References

1. G. T. Fallis, *Walking Toy.* U.S. Patent No. 376588 (United States Patent Office, Alexandria, VA, 1888).
2. T. McGeer, "Passive dynamic walking," *Int. J. Robot. Res.* **9**, 62–82 (1990).
3. T. McGeer, "Passive dynamic walking with knees," *Proc. IEEE Conf. Robot. Autom.* **2**, 1640–1645 (1990).
4. M. Garcia, A. Chatterjee, A. Ruina and M. Coleman, "The simplest walking model: Stability, complexity, and scaling," *J. Biomech. Eng.* **120**(2), 281–288 (1998).
5. A. Goswami, B. Thuilot and B. Espiau, "A study of the passive gait of a compass-like biped robot: Symmetry and chaos," *Int. J. Robot. Res.* **17**, 1282–1301 (1998).
6. M. J. Kurz, T. N. Judkins, C. Arellano and M. Scott-Pandorf, "A passive dynamic walking robot that has a deterministic nonlinear gait," *J. Biomech.* **40**(4), 617–656 (2008).
7. M. J. Coleman and A. Ruina, "An uncontrolled walking toy that cannot stand still," *Phys. Rev. Lett.* **80**(16), 36–58 (1998).
8. A. D. Kuo, "Stabilization of lateral motion in passive dynamic walking," *Int. J. Robot. Res.* **18**, 917–930 (1999).
9. M. Wisse, A. L. Schwab and R. Q. V. Linde, "A 3D passive dynamic biped with yaw and roll compensation," *Robotica* **19**(03), 275 (2001).
10. S. H. Collins, M. Wisse and A. Ruina, "A three-dimensional passive-dynamic walking robot with two legs and knees," *Int. J. Robot. Res.* **20**, 607–615 (2001).
11. T. Narukawa, K. Yokoyama, M. Takahashi and K. Yoshida, "A Simple 3D Straight-Legged Passive Walker with Flat Feet and Ankle Springs," *IEEE/RSJ International Conference on Intelligent Robots and Systems, 2008 (IROS 2008)* pp. 2952–2957.
12. M. Wisse, A. L. Schwab and F. C. T. van der Helm, "Passive dynamic walking model with upper body," *Robotica* **22**(06), 681 (2004).
13. A. T. Safa, M. G. Saadat and M. Naraghi, "Passive dynamic of the simplest walking model: Replacing ramps with stairs," *Mech. Mach. Theory* **40**(7), 1027–1034 (2007).

https://doi.org/10.1017/S0263574710000779 Published online by Cambridge University Press

14. L. Ning, L. Junfeng and W. Tianshu, "The effects of parameter variation on the gaits of passive walking models: Simulations and experiments," *Robotica* **27**(04), 511–528 (2009).
15. http://world.honda.com/ASIMO/
16. K. L. Johnson, *Contact Mechanics* (Cambridge University Press, Cambridge, UK, 1985).
17. http://www.mscsoftware.com/support/prod_support/mdadams/MDR2/mdadams_r2_doc_install.pdf
18. T. McGeer, "Passive bipedal running," *R. Soc. Lond. Proc. Ser.* B **240**, 107–134 (1990).
19. Q. Wu and N. Sabet, "An experimental study of passive dynamic walking," *Robotica* **22**(3), 251 (2004).

https://doi.org/10.1017/S0263574710000779 Published online by Cambridge University Press